

Simulation of turn-by-turn passage of protons through the H-minus stripping foil in booster

C. Gardner

July 2017

Collider Accelerator Department
Brookhaven National Laboratory

U.S. Department of Energy

USDOE Office of Science (SC), Nuclear Physics (NP) (SC-26)

Notice: This technical note has been authored by employees of Brookhaven Science Associates, LLC under Contract No. DE-SC0012704 with the U.S. Department of Energy. The publisher by accepting the technical note for publication acknowledges that the United States Government retains a non-exclusive, paid-up, irrevocable, world-wide license to publish or reproduce the published form of this technical note, or allow others to do so, for United States Government purposes.

DISCLAIMER

This report was prepared as an account of work sponsored by an agency of the United States Government. Neither the United States Government nor any agency thereof, nor any of their employees, nor any of their contractors, subcontractors, or their employees, makes any warranty, express or implied, or assumes any legal liability or responsibility for the accuracy, completeness, or any third party's use or the results of such use of any information, apparatus, product, or process disclosed, or represents that its use would not infringe privately owned rights. Reference herein to any specific commercial product, process, or service by trade name, trademark, manufacturer, or otherwise, does not necessarily constitute or imply its endorsement, recommendation, or favoring by the United States Government or any agency thereof or its contractors or subcontractors. The views and opinions of authors expressed herein do not necessarily state or reflect those of the United States Government or any agency thereof.

C-A/AP/588

July 2017

Simulation of turn-by-turn passage of protons through the H-minus stripping foil in Booster

C.J. Gardner



Collider-Accelerator Department
Brookhaven National Laboratory
Upton, N.Y. 11973

U.S. Department of Energy
Office of Science, Office of Nuclear Physics

Notice: This document has been authorized by employees of Brookhaven Science Associates, LLC under Contract No. **DE-SC0012704** with the U.S. Department of Energy. The United States Government retains a non-exclusive, paid-up, irrevocable, world-wide license to publish or reproduce the published form of this document, or allow others to do so, for United States Government purposes.

DISCLAIMER

This report was prepared as an account of work sponsored by an agency of the United States Government. Neither the United States Government nor any agency thereof, nor any of their employees, nor any of their contractors, subcontractors, or their employees, makes any warranty, express or implied, or assumes any legal liability or responsibility for the accuracy, completeness, or any third party's use or the results of such use of any information, apparatus, product, or process disclosed, or represents that its use would not infringe privately owned rights. Reference herein to any specific commercial product, process, or service by trade name, trademark, manufacturer, or otherwise, does not necessarily constitute or imply its endorsement, recommendation, or favoring by the United States Government or any agency thereof or its contractors or subcontractors. The views and opinions of authors expressed herein do not necessarily state or reflect those of the United States Government or any agency thereof.

Simulation of Turn-by-Turn Passage of Protons through the H-minus Stripping Foil in Booster

C.J. Gardner

July 6, 2017

Equations for transverse emittance growth due to multiple passes of circulating proton beam through the H-minus stripping foil in Booster were developed in [1]. These were based on simple principles of statistics and simple assumptions about the initial distribution of particles incident on the foil. It was assumed there that the foil dimensions and position of the incoming beam are such that all particles hit the foil on every turn around the machine. In the present note we assume only that all incoming H-minus ions from Linac hit the foil and are stripped of their electrons. The resulting protons circulate indefinitely around the machine. Setups in which the foil width is reduced so that not all protons hit the foil on every turn are studied here by simulation. The aim is to determine the effectiveness of such setups in reducing the emittance growth of circulating proton beam during the injection of H-minus beam. The simulations also serve as a check of the equations developed in [1], and vice versa.

The particulars of the simulation setup are given in Sections 1 through 11.

Figures 1 through 12 show simulation results for the case in which all particles hit the foil on every turn. The results are in good agreement with those obtained from the equations of reference [1].

Figures 13 through 19 show simulation results for various setups in which the foil width is reduced. These results are summarized in Section 12.

In all figures the horizontal axis gives the turn number. The unit of the vertical axis is micrometers (μm) in all plots of emittance.

1 Turn-by-Turn Positions and Angles

Let X_{ni} and X'_{ni} be the horizontal position and angle (with respect to the closed orbit) of the i th particle just upstream of the foil on the n th turn around the machine. Then the position and angle on the next turn (again just upstream of the foil) are given by

$$\begin{pmatrix} X_{mi} \\ X'_{mi} \end{pmatrix} = \begin{pmatrix} C + \alpha S & \beta S \\ -\gamma S & C - \alpha S \end{pmatrix} \begin{pmatrix} X_{ni} \\ X'_{ni} + \phi_{ni} \end{pmatrix} \quad (1)$$

where

$$m = n + 1 \quad (2)$$

and ϕ_{ni} is the angular kick received by the i th particle as it passes through the foil on the n th turn. Here α , β , γ are the Courant-Snyder parameters of the machine lattice at the foil. These satisfy

$$\beta\gamma = 1 + \alpha^2. \quad (3)$$

The parameters C and S are

$$C = \cos 2\pi Q, \quad S = \sin 2\pi Q \quad (4)$$

where Q is the machine tune.

Carrying out the matrix multiplication in (1) gives

$$X_{mi} = (C + \alpha S)X_{ni} + \beta S X'_{ni} + \beta S \phi_{ni} \quad (5)$$

$$X'_{mi} = -\gamma S X_{ni} + (C - \alpha S)(X'_{ni} + \phi_{ni}) \quad (6)$$

which, with the help of (3), can be written as

$$X_{mi} = C X_{ni} + S(\alpha X_{ni} + \beta X'_{ni}) + S\beta\phi_{ni} \quad (7)$$

$$\alpha X_{mi} + \beta X'_{mi} = -S X_{ni} + C(\alpha X_{ni} + \beta X'_{ni}) + C\beta\phi_{ni}. \quad (8)$$

Defining new coordinates

$$Y_{ni} = \alpha X_{ni} + \beta X'_{ni} \quad (9)$$

$$Y_{mi} = \alpha X_{mi} + \beta X'_{mi} \quad (10)$$

we then have

$$X_{mi} = C X_{ni} + S Y_{ni} + S\beta\phi_{ni} \quad (11)$$

$$Y_{mi} = -S X_{ni} + C Y_{ni} + C\beta\phi_{ni}. \quad (12)$$

These are the turn-by-turn equations used in the simulation. The particles are tracked for 333 turns, which corresponds to a time interval of 396 microseconds for protons with a kinetic energy of 200 MeV.

2 Foil Setups

It is assumed that the initial beam distribution is centered on the closed orbit at the foil. The simulation code then provides **three setups** for the extent of the foil:

1. Foil extends from $-\mathcal{A}$ to $+\mathcal{A}$ in the horizontal and vertical planes, where \mathcal{A} is the half-aperture of the beam pipe.
2. Foil extends from $-\mathcal{A}$ to $\mathcal{C} + L$ in the horizontal plane and from $-\mathcal{A}$ to $+\mathcal{A}$ in the vertical plane. Here \mathcal{C} is the horizontal position of the closed orbit at the foil and $L > 0$.
3. Foil extends from $\mathcal{C} - L$ to $\mathcal{C} + L$ in the horizontal plane and from $-\mathcal{A}$ to $+\mathcal{A}$ in the vertical plane.

Under **Setup 1**, all particles pass through the foil on every turn. In this case the simulation uses equations (11) and (12) as written.

Under **Setup 2**, the simulation sets $\phi_{ni} = 0$ in (11) and (12) whenever $X_{ni} > L$.

Under **Setup 3**, the simulation sets $\phi_{ni} = 0$ in (11) and (12) whenever $X_{ni} > L$, or $X_{ni} < -L$.

Since all particles pass through the foil on every turn under setup 1, the simulation under this setup gives the emittance growth in both the horizontal and vertical planes. Simulations under setups 2 and 3 apply to motion in the **horizontal plane only**.

3 Single Particle Emittance

The Courant-Snyder invariant associated with X_{ni} and X'_{ni} is

$$E_{ni} = \gamma X_{ni}^2 + 2\alpha X_{ni} X'_{ni} + \beta X_{ni}'^2 \quad (13)$$

which we can write as

$$E_{ni} = \frac{1}{\beta} \left\{ X_{ni}^2 + (\alpha X_{ni} + \beta X'_{ni})^2 \right\}. \quad (14)$$

Using (9), we then have

$$\beta E_{ni} = X_{ni}^2 + Y_{ni}^2. \quad (15)$$

Although the area of the ellipse defined by (13) is πE_{ni} , we define the emittance of the i th particle on the n th turn around the machine to be

$$E_{ni} = \frac{1}{\beta} \{X_{ni}^2 + Y_{ni}^2\}. \quad (16)$$

This is consistent with current convention.

4 Averages

The averages of interest for each turn are

$$\langle X_n \rangle = \frac{1}{M} \sum_{i=1}^M X_{ni}, \quad \langle Y_n \rangle = \frac{1}{M} \sum_{i=1}^M Y_{ni} \quad (17)$$

$$\langle X_n^2 \rangle = \frac{1}{M} \sum_{i=1}^M X_{ni}^2, \quad \langle Y_n^2 \rangle = \frac{1}{M} \sum_{i=1}^M Y_{ni}^2 \quad (18)$$

and

$$\langle X_n Y_n \rangle = \frac{1}{M} \sum_{i=1}^M X_{ni} Y_{ni} \quad (19)$$

where

$$M = 9,999,999 \quad (20)$$

is the number of particles in the distribution. The averages are calculated turn by turn in the simulation.

As already mentioned, it is assumed that the initial beam distribution is centered on the closed orbit at the foil. This ensures that (to a very good approximation)

$$\langle X_n \rangle = 0, \quad \langle Y_n \rangle = 0 \quad (21)$$

for all turns.

5 Emittance of Distribution

The **average emittance** of the distribution on the n th turn is

$$\langle E_n \rangle = \frac{1}{\beta} \left\{ \langle X_n^2 \rangle + \langle Y_n^2 \rangle \right\}. \quad (22)$$

The **emittance** of the distribution on the n th turn is defined to be

$$\mathcal{E}_n = \frac{1}{\beta} \langle X_n^2 \rangle. \quad (23)$$

If the distribution is **Gaussian** with density

$$\rho(X, Y) = \left(\frac{1}{2\pi\mathcal{E}_n\beta} \right) \exp \left\{ -\frac{X^2 + Y^2}{2\mathcal{E}_n\beta} \right\} \quad (24)$$

then the emittance that contains fraction [2]

$$F = 1 - e^{-3} = 0.9502 \quad (25)$$

of the particles is $6\mathcal{E}_n$. This is called the **95 percent emittance**.

The above emittances are un-normalized. Normalized emittances are obtained by multiplying the un-normalized ones by the relativistic factor $\beta\gamma = 0.68684$ for 200 MeV protons. Thus the **normalized 95 percent emittance** is

$$(6\mathcal{E}_n)_N = 0.68684 (6\mathcal{E}_n). \quad (26)$$

6 Symmetry of Distribution

We also define dimensionless parameters

$$\Delta_n = \frac{\langle X_n^2 \rangle - \langle Y_n^2 \rangle}{\langle X_n^2 \rangle + \langle Y_n^2 \rangle}, \quad K_n = \frac{\langle X_n Y_n \rangle}{\langle X_n^2 \rangle + \langle Y_n^2 \rangle} \quad (27)$$

which are measures of the symmetry (or asymmetry) of the distribution as discussed in [1]. The distribution is **symmetric** on the n th turn if

$$\Delta_n = 0, \quad K_n = 0. \quad (28)$$

7 Initial Distribution

We assume that the initial distribution of particles is **Gaussian** with density

$$\rho(X_0, Y_0) = P(X_0)P(Y_0) \quad (29)$$

where

$$P(Z) = \left(\frac{1}{2\pi\mathcal{E}_0\beta} \right)^{1/2} \exp \left\{ -\frac{Z^2}{2\mathcal{E}_0\beta} \right\}. \quad (30)$$

We then have

$$\langle X_0 \rangle = \langle Y_0 \rangle = \int_{-\infty}^{+\infty} ZP(Z) dZ \quad (31)$$

$$\langle X_0^2 \rangle = \langle Y_0^2 \rangle = \int_{-\infty}^{+\infty} Z^2 P(Z) dZ \quad (32)$$

and

$$\langle X_0 Y_0 \rangle = \int_{-\infty}^{+\infty} X P(X) dX \int_{-\infty}^{+\infty} Y P(Y) dY. \quad (33)$$

The definite integrals

$$\int_{-\infty}^{+\infty} x e^{-a^2 x^2} dx = 0, \quad \int_{-\infty}^{+\infty} x^2 e^{-a^2 x^2} dx = \frac{\sqrt{\pi}}{2a^3} \quad (34)$$

then give

$$\langle X_0 \rangle = \langle Y_0 \rangle = 0 \quad (35)$$

$$\langle X_0^2 \rangle = \langle Y_0^2 \rangle = \mathcal{E}_0\beta \quad (36)$$

and

$$\langle X_0 Y_0 \rangle = 0. \quad (37)$$

The initial distribution is therefore symmetric with emittance

$$\frac{1}{\beta} \langle X_0^2 \rangle = \mathcal{E}_0. \quad (38)$$

In the simulation we set

$$\underline{\mathcal{E}_0 = 0.6 \mu\text{m}} \quad (39)$$

and

$$\underline{\beta = 5 \text{ meters.}} \quad (40)$$

The Numerical Recipes routine **gasdev** [3] then produces an initial distribution that is symmetric and Gaussian with

$$\langle X_0^2 \rangle = \frac{1}{M} \sum_{i=1}^M X_{0i} = \mathcal{E}_0 \beta \quad (41)$$

$$\langle Y_0^2 \rangle = \frac{1}{M} \sum_{i=1}^M Y_{0i} = \mathcal{E}_0 \beta. \quad (42)$$

The normalized 95 percent emittance for the set value of \mathcal{E}_0 is

$$(6\mathcal{E}_0)_N = \underline{2.47 \mu\text{m}} \quad (43)$$

which is consistent with recent measurements of the Linac beam. The corresponding beam half-width at the foil is

$$\sqrt{\beta (6\mathcal{E}_0)} = \underline{4.24 \text{ mm}}. \quad (44)$$

8 Distribution of Angular Kicks from Foil

We assume that the distribution of angular kicks received by particles as they pass through the foil is also **Gaussian** with probability density

$$\rho(\phi) = \left(\frac{1}{2\pi\sigma^2} \right)^{1/2} \exp\left(-\frac{\phi^2}{2\sigma^2} \right). \quad (45)$$

Using the second of equations (34) we then have

$$\langle \phi^2 \rangle = \int_{-\infty}^{+\infty} \phi^2 \rho(\phi) d\phi = \sigma^2. \quad (46)$$

The root mean square (rms) angular kick received by the particles on any given turn is then

$$\langle \phi^2 \rangle^{1/2} = \sigma. \quad (47)$$

In the simulation, the value of σ is specified and the Numerical Recipes routine **gasdev** [3] produces a distribution of kicks that is Gaussian with

$$\langle \phi^2 \rangle^{1/2} = \left\{ \frac{1}{M} \sum_{i=1}^M \phi_i^2 \right\}^{1/2} = \sigma. \quad (48)$$

Here ϕ_i is the angular kick received by the i th particle on a given turn.

The analysis carried out in [1] shows that

$$\langle \phi^2 \rangle^{1/2} = 0.0344, 0.0297, 0.0243, 0.0165 \text{ mrad} \quad (49)$$

for 200 MeV protons incident on 200, 150, 100, and 50 microgram per cm² carbon foils, respectively. In the simulation we set

$$\sigma = 0.0344 \text{ and } 0.0243 \text{ mrad} \quad (50)$$

for the 200 and 100 microgram per cm² carbon foils, respectively.

9 Expected Emittance

For a sufficiently large number of particles we expect the emittance \mathcal{E}_n obtained by simulation under foil setup 1 to be in good agreement with that obtained from equation (154) of [1]. From that equation we have expected emittance

$$\mathcal{E}_n = \mathcal{E}_0 + \frac{1}{2} (n - \mathcal{A}_n) \beta \langle \phi^2 \rangle \quad (51)$$

$$\mathcal{A}_n = \frac{\mathcal{S}_1 \mathcal{S}_n}{2(1 - \mathcal{C}_1)} - \frac{1}{2} (1 - \mathcal{C}_n) \quad (52)$$

and

$$\mathcal{C}_n = \cos 2n\psi, \quad \mathcal{S}_n = \sin 2n\psi, \quad \psi = 2\pi Q. \quad (53)$$

The expected average

$$\langle E_n \rangle = 2\mathcal{E}_0 + n\beta \langle \phi^2 \rangle \quad (54)$$

is given by equations (155) and (159) of [1].

10 Expected Δ_n and K_n Terms

Similarly, equations (180) and (181) of [1] are

$$\frac{\langle X_n^2 - Y_n^2 \rangle}{\langle X_n^2 + Y_n^2 \rangle} = -\frac{\mathcal{A}_n}{\langle E_n \rangle} \beta \langle \phi^2 \rangle \quad (55)$$

and

$$\frac{2 \langle X_n Y_n \rangle}{\langle X_n^2 + Y_n^2 \rangle} = -\frac{\mathcal{B}_n}{\langle E_n \rangle} \beta \langle \phi^2 \rangle \quad (56)$$

where

$$\langle E_n \rangle = 2\mathcal{E}_0 + n\beta \langle \phi^2 \rangle \quad (57)$$

$$\mathcal{A}_n = \frac{\mathcal{S}_1 \mathcal{S}_n}{2(1 - \mathcal{C}_1)} - \frac{1}{2} (1 - \mathcal{C}_n) \quad (58)$$

$$\mathcal{B}_n = -\frac{\mathcal{S}_n}{2} - \frac{\mathcal{S}_1 (1 - \mathcal{C}_n)}{2(1 - \mathcal{C}_1)} \quad (59)$$

and

$$\mathcal{C}_n = \cos 2n\psi, \quad \mathcal{S}_n = \sin 2n\psi, \quad \psi = 2\pi Q. \quad (60)$$

This gives expected values

$$\Delta_n = -\frac{\mathcal{A}_n}{\langle E_n \rangle} \beta \langle \phi^2 \rangle \quad (61)$$

and

$$2K_n = -\frac{\mathcal{B}_n}{\langle E_n \rangle} \beta \langle \phi^2 \rangle. \quad (62)$$

11 Machine Tunes

As reported in [4, 5] the tunes in Booster are set to be just above 4.5 during the injection of polarized protons. This is done so that the half-integer stopband correction scheme can be employed to reduce the lattice beta at the foil. In the simulations discussed here the fractional part of the machine tune is taken to be

$$Q = 0.54. \quad (63)$$

12 Summary

Simulations have been carried out to study setups in which the width of the H-minus stripping foil is reduced in Booster. The aim was to determine the effectiveness of such setups in reducing the emittance growth of circulating proton beam during the injection of H-minus beam. Three setups were studied:

1. Foil extends from $-\mathcal{A}$ to $+\mathcal{A}$ in the horizontal and vertical planes, where \mathcal{A} is the half-aperture of the beam pipe. In this case all particles pass through the foil on every turn around the machine. This produces the largest emittance growth of the three setups. The results are in agreement with those obtained from the equations of reference [1].
2. Foil extends from $-\mathcal{A}$ to $\mathcal{C} + L$ in the horizontal plane and from $-\mathcal{A}$ to $+\mathcal{A}$ in the vertical plane. Here \mathcal{C} is the horizontal position of the closed orbit at the foil and $L > 0$. The incoming H-minus beam is centered on \mathcal{C} , and L is set to be the initial beam half-width (4.2 mm) at the foil. In this case the incoming H-minus beam fits completely on the foil, but the edge of the beam is up against the foil edge at $\mathcal{C} + L$. Particles with position (with respect to closed orbit) $X_n > L$ miss the foil on the n th turn around the machine.
3. Foil extends from $\mathcal{C} - L$ to $\mathcal{C} + L$ in the horizontal plane and from $-\mathcal{A}$ to $+\mathcal{A}$ in the vertical plane. Here again \mathcal{C} is the horizontal position of the closed orbit at the foil and $L > 0$. The incoming H-minus beam is again centered on \mathcal{C} , and L is set to be the initial beam half-width (4.2 mm) at the foil. In this case the incoming beam just fits on the foil. Particles hit the foil on the n th turn only if $-L \leq X_n \leq L$. This produces the smallest emittance growth of the three setups. The final emittance obtained under setup 2 is approximately halfway between the final emittances obtained under setups 1 and 3.

Since all particles pass through the foil on every turn under setup 1, the simulation under this setup gives the emittance growth in both the horizontal and vertical planes. Simulations under setups 2 and 3 apply to motion in the horizontal plane only. An upper limit on the growth in the vertical plane in this case is given by the growth obtained under setup 1.

In the simulations, the initial normalized 95% emittance was taken to be $2.47 \mu\text{m}$, which is consistent with recent measurements of the Linac beam.

This gives a beam half-width of 4.2 mm at the foil. The surface density of the carbon stripping foil was taken to be either 200 or 100 micrograms per cm^2 . These are the surface densities that have been used in practice for polarized proton operation in Booster.

For the 200 microgram per cm^2 foil, the final emittances (normalized 95%) obtained after 333 turns under setups 1, 2, and 3 are 6.56, 6.42, and 6.28 μm respectively. The corresponding growths in emittance are 4.09, 3.95, and 3.81 μm respectively.

For the 100 microgram per cm^2 foil, the final emittances (normalized 95%) obtained after 333 turns under setups 1 and 3 are 4.51 and 4.43 μm respectively. The corresponding growths in emittance are 2.04 and 1.96 μm respectively.

Here one sees that the emittance growth obtained with the 100 microgram per cm^2 foil under setup 1 is half that obtained with the 200 microgram per cm^2 foil. It is for this reason that only the 100 microgram per cm^2 foil has been used in recent years for polarized proton operation in Booster. Foils thinner than 100 micrograms per cm^2 have not been used. These are fragile, and the fraction of neutral H atoms or unstripped H-minus ions emerging from them is high enough to cause concern for machine components downstream.

One also sees that the reduction in final emittance achieved in going from setup 1 to setup 3 is small compared to the emittance itself. The conclusion is that the special foil described in setup 3 is not really necessary; an ordinary foil like the one described in setup 2 is all that is needed. This setup has the advantage that with the incoming beam placed up against the foil edge, one can quickly move the circulating proton beam off the foil at the end of H-minus injection.

The simulations discussed in this note are strictly two-dimensional. (The two coordinates are X and $Y = \alpha X + \beta X'$, where X and X' are the horizontal position and angle with respect to the closed orbit.) For setups involving a foil that has its width reduced in both the horizontal and vertical planes, a four-dimensional simulation is required. Such a foil has been used during polarized proton operation in Booster. It is called the “Stamp” foil and is described in [5]. To date there is no definitive measurement of emittance growth in Booster showing that this foil is any better at reducing emittance growth than one with the width reduced only in the horizontal plane as in setup 3.

References

- [1] C.J. Gardner, “Emittance Growth due to Multiple Passes through the H-minus Stripping Foil in Booster”, C-A/AP/Note 583, March, 2017
- [2] C.J. Gardner, C-A/AP/Note 583, March, 2017, p. 23.
- [3] W.H. Press, et al, “Numerical Recipes in FORTRAN”, Second Edition, Cambridge University Press, 1992
- [4] K.L. Zeno, “An Overview of Booster and AGS Polarized Proton Operation during Run 15”, C-A/AP/Note 552, October, 2015
- [5] K.A. Brown, et al, “Minimizing Emittance Growth during H-minus Injection in the AGS Booster”, Proceedings of PAC09, Vancouver, BC, Canada, pp. 3729–3731.

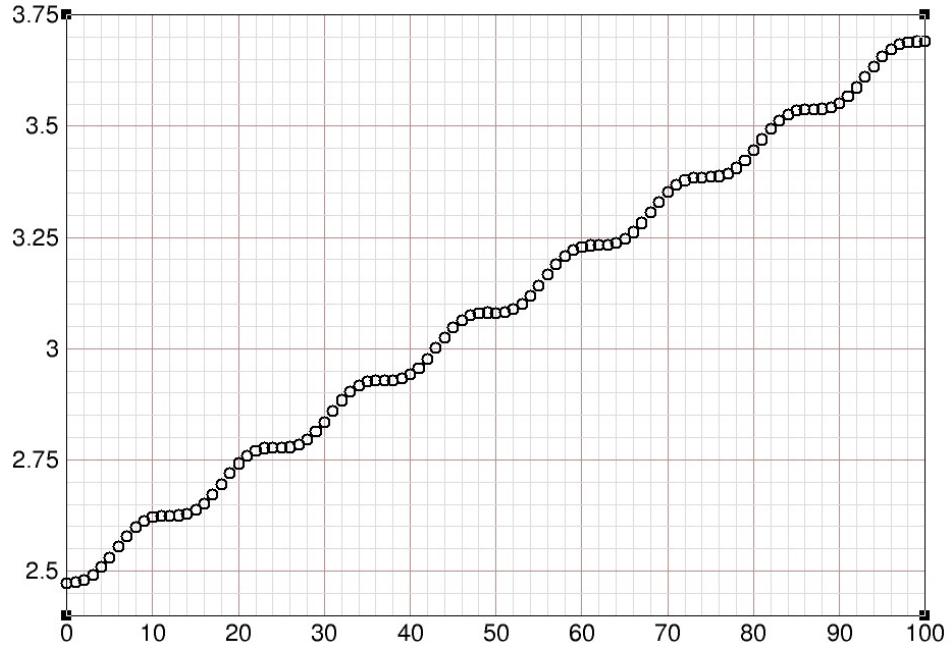


Figure 1: Turn-by-turn values of the normalized 95% emittance $(6\mathcal{E}_n)_N$ obtained by simulation under foil setup 1. The horizontal axis gives the turn number n . The units of the vertical axis are μm . The initial emittance $(6\mathcal{E}_0)_N = 2.47 \mu\text{m}$. The surface density of the carbon foil is 200 microgram per cm^2 . The tune $Q = 0.54$.

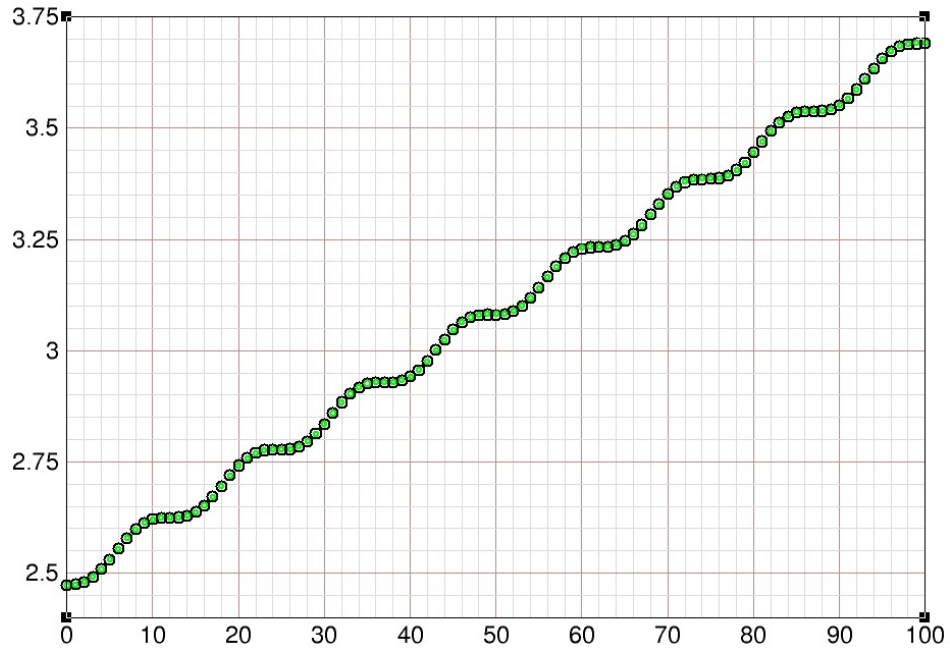


Figure 2: Same as previous figure, but with the addition of the expected values (green dots) of $(6\mathcal{E}_n)_N$ under foil setup 1. As can be seen, there is very good agreement between the simulation (black circles) and expected values. The expected values are defined in Section 9.

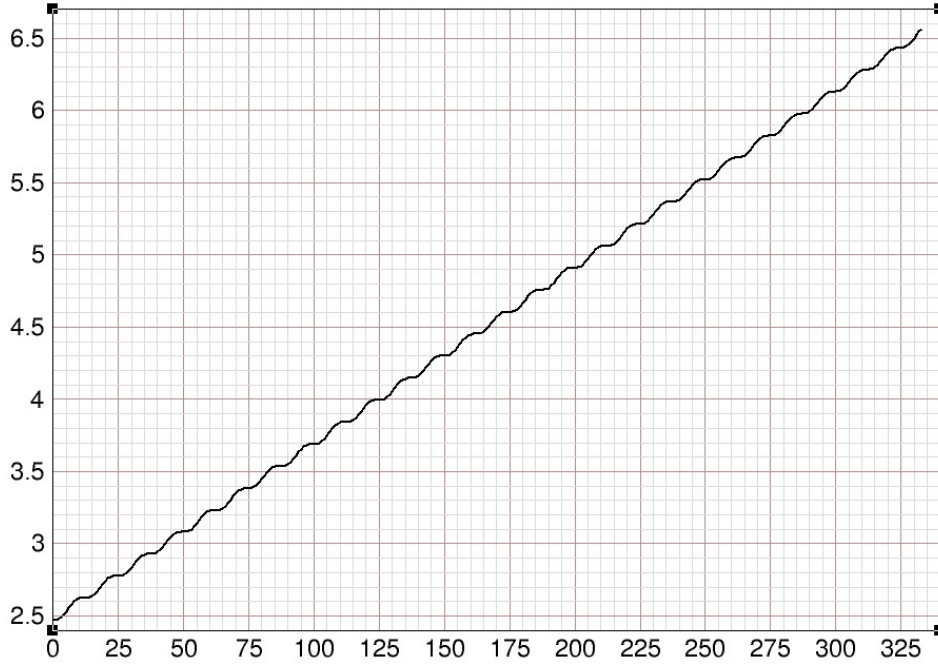


Figure 3: Turn-by-turn values of the normalized 95% emittance $(6\mathcal{E}_n)_N$ obtained by simulation under foil setup 1 with the simulation extended to 333 turns. The horizontal axis gives the turn number n . The units of the vertical axis are μm . The initial emittance $(6\mathcal{E}_0)_N = 2.47 \mu\text{m}$. The final emittance $(6\mathcal{E}_n)_N = 6.56 \mu\text{m}$. The emittance growth over 333 turns is then $(6\mathcal{E}_n - 6\mathcal{E}_0)_N = 4.09 \mu\text{m}$. The surface density of the carbon foil is 200 microgram per cm^2 . The tune $Q = 0.54$.

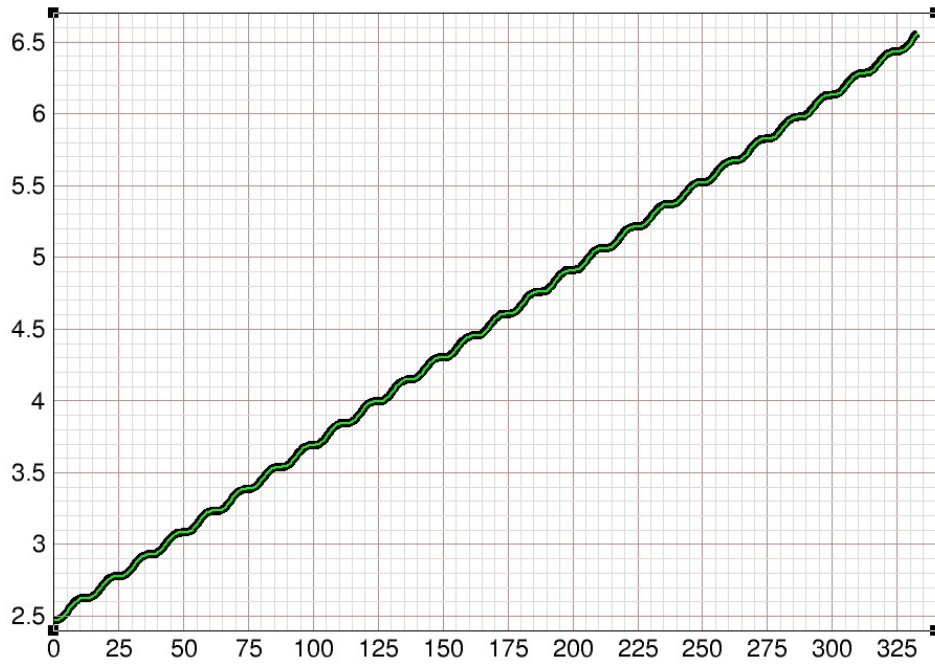


Figure 4: Same as previous figure, but with the addition of the expected values (green curve) of $(6\mathcal{E}_n)_N$ under foil setup 1. As can be seen, there is very good agreement between the simulation (black curve) and expected values.

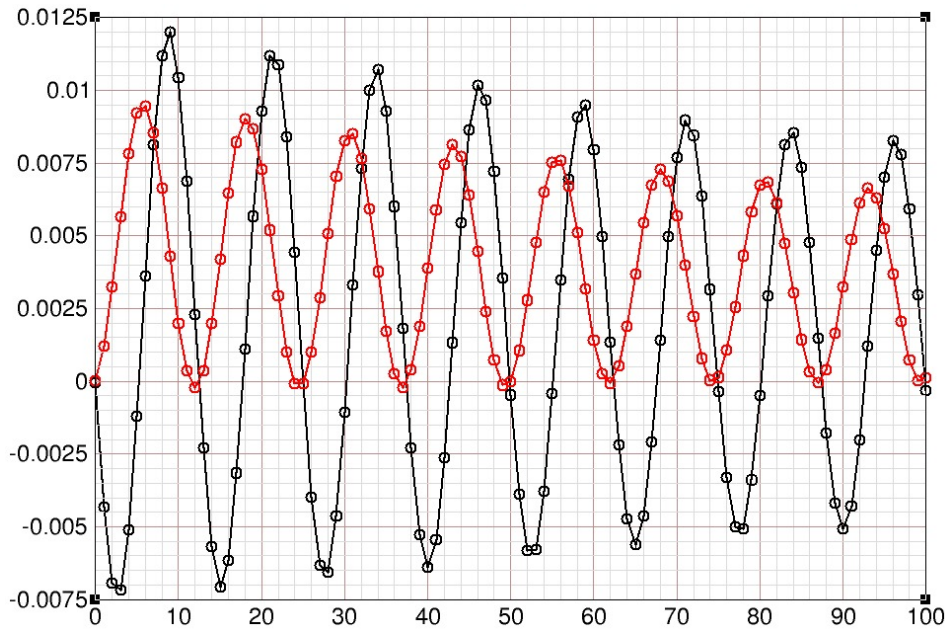


Figure 5: Simulation values of dimensionless parameters Δ_n (black circles) and K_n (red circles) obtained under foil setup 1. These are the symmetry parameters defined in Section 6. The horizontal axis gives the turn number n . The initial normalized 95% emittance is $(6\mathcal{E}_0)_N = 2.47 \mu\text{m}$. The surface density of the carbon foil is 200 microgram per cm^2 . The tune $Q = 0.54$.

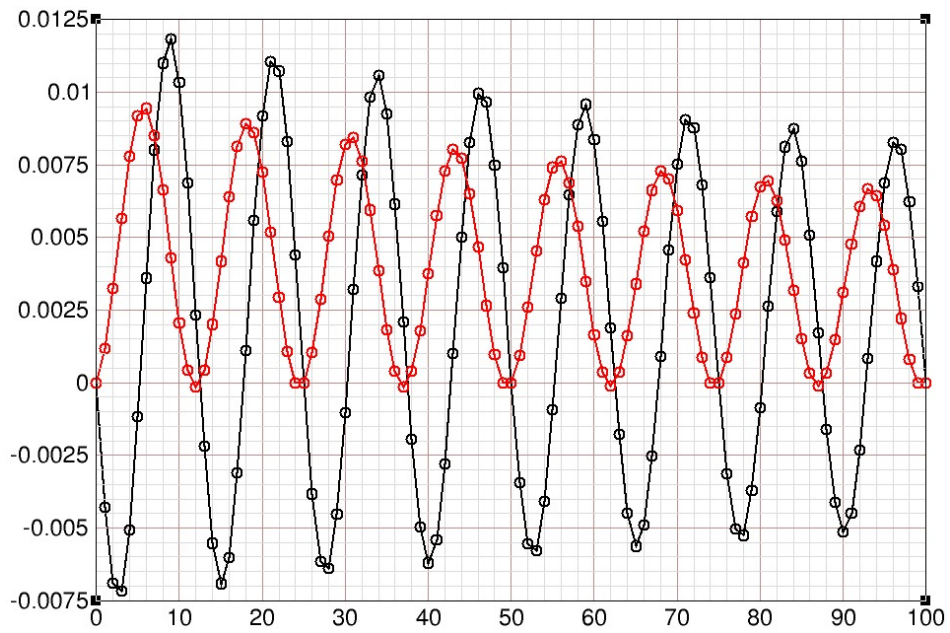


Figure 6: Expected values of Δ_n (black circles) and K_n . These are in good agreement with the simulation values in the previous figure. The expected values are defined in Section 10.

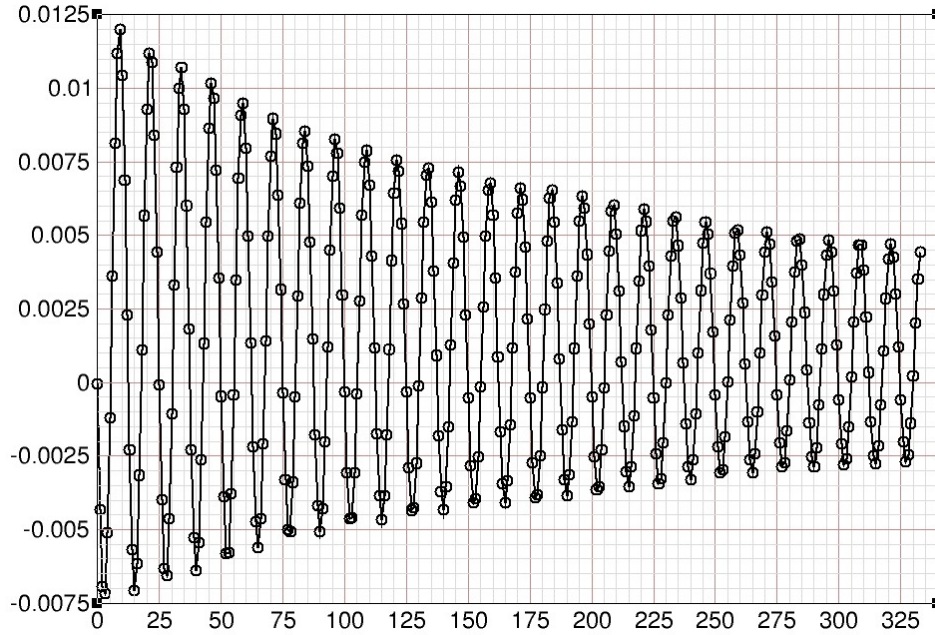


Figure 7: Simulation values of dimensionless symmetry parameter Δ_n obtained under foil setup 1 with the simulation extended to 333 turns. The horizontal axis gives the turn number n . The initial normalized 95% emittance is $(6\mathcal{E}_0)_N = 2.47 \mu\text{m}$. The surface density of the carbon foil is 200 microgram per cm^2 . The tune $Q = 0.54$.

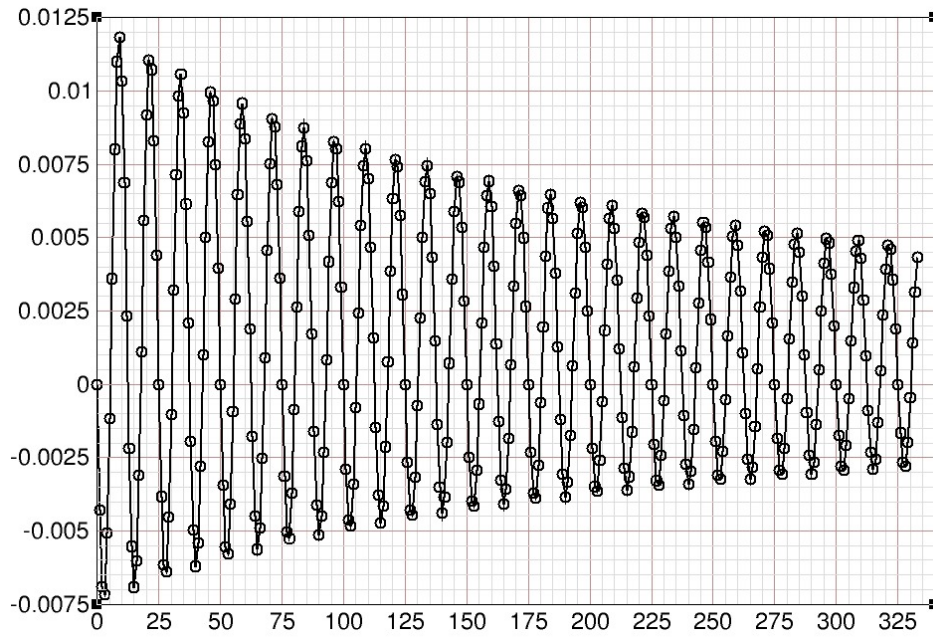


Figure 8: Expected values of Δ_n . These are in good agreement with the simulation values in the previous figure.

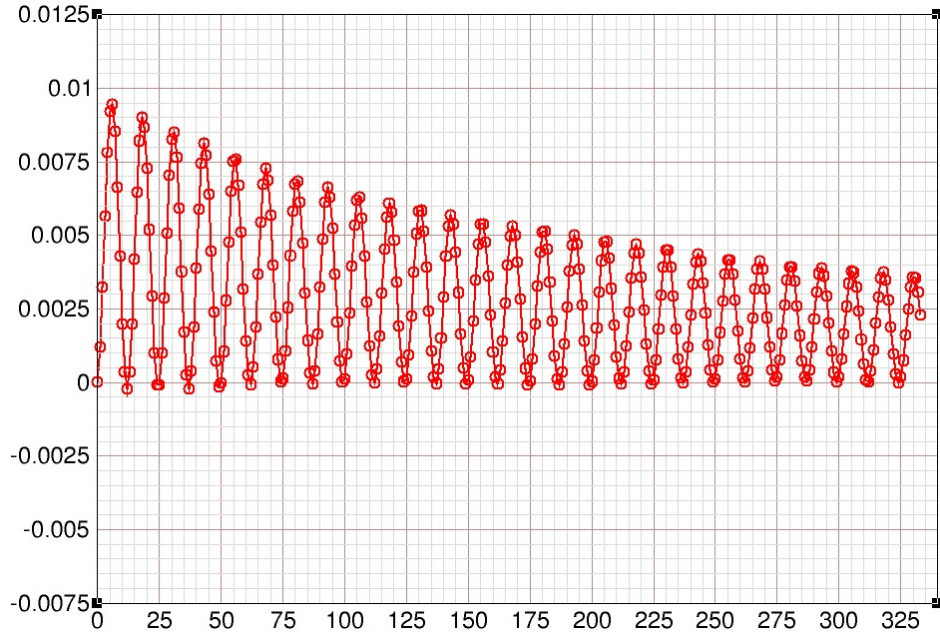


Figure 9: Simulation values of dimensionless symmetry parameter K_n obtained under foil setup 1 with the simulation extended to 333 turns. The horizontal axis gives the turn number n . The initial normalized 95% emittance is $(6\mathcal{E}_0)_N = 2.47 \mu\text{m}$. The surface density of the carbon foil is 200 microgram per cm^2 . The tune $Q = 0.54$.

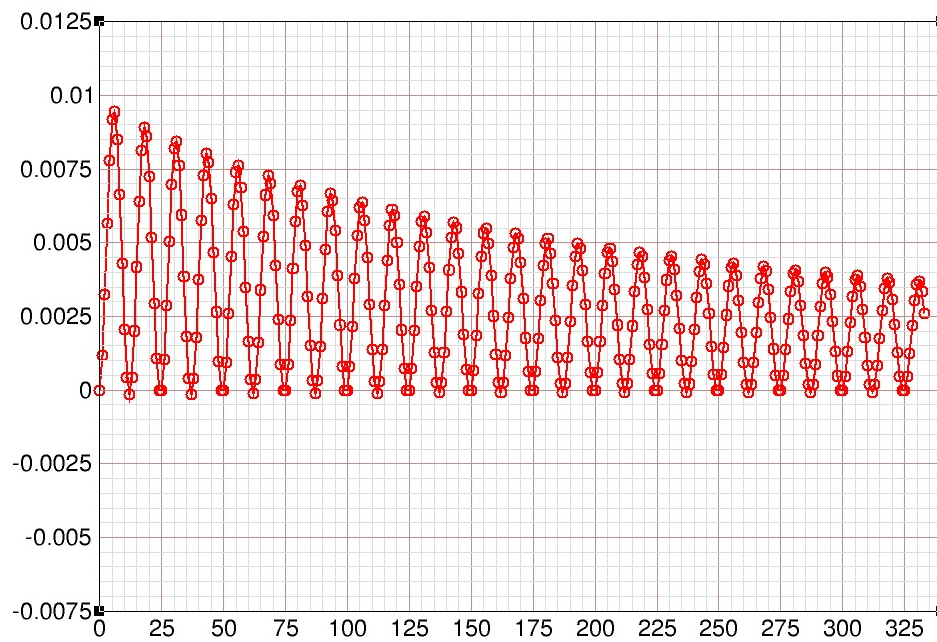


Figure 10: Expected values of K_n . These are in good agreement with the simulation values in the previous figure.

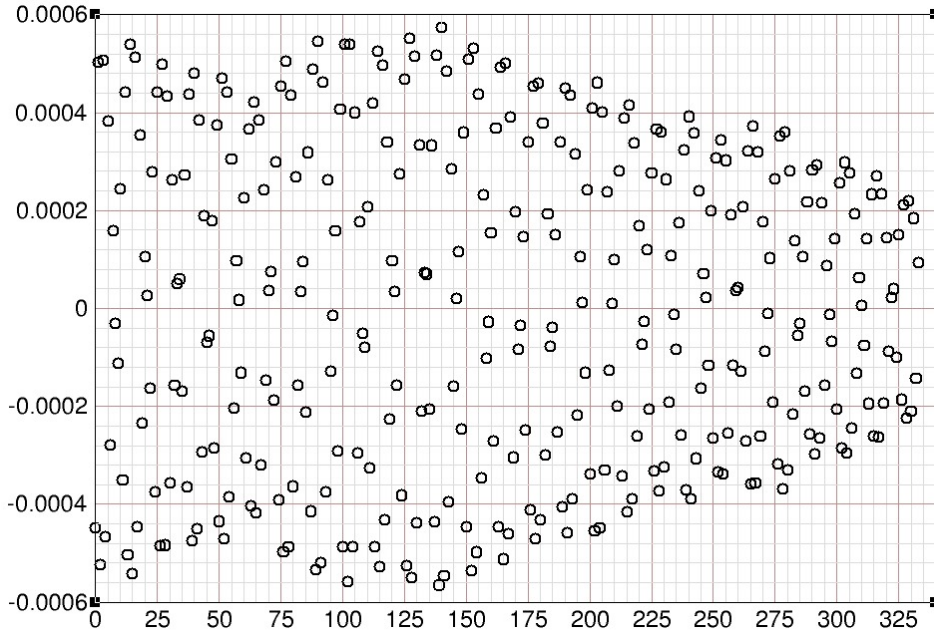


Figure 11: Simulation values of normalized averages $\langle X_n \rangle / \sqrt{\langle E_n \rangle} \beta$ obtained under foil setup 1. These are dimensionless and very close to zero as expected. The horizontal axis gives the turn number n . The initial normalized 95% emittance is $(6\mathcal{E}_0)_N = 2.47 \mu\text{m}$. The surface density of the carbon foil is 200 microgram per cm^2 . The tune $Q = 0.54$.

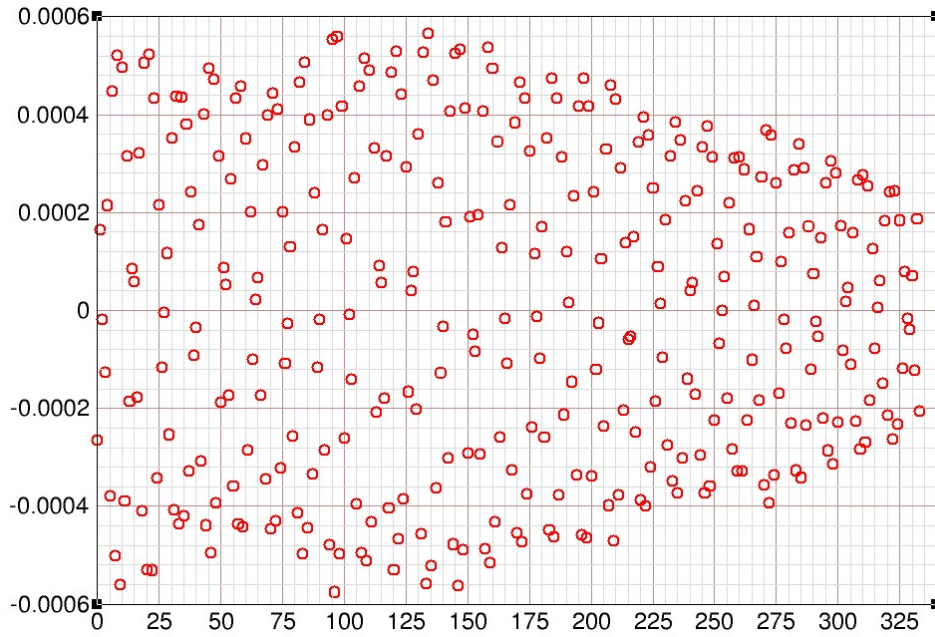


Figure 12: Simulation values of normalized averages $\langle Y_n \rangle / \sqrt{\langle E_n \rangle} \beta$ obtained under foil setup 1. These are dimensionless and very close to zero as expected. The horizontal axis gives the turn number n . The initial normalized 95% emittance is $(6\mathcal{E}_0)_N = 2.47 \mu\text{m}$. The surface density of the carbon foil is 200 microgram per cm^2 . The tune $Q = 0.54$.

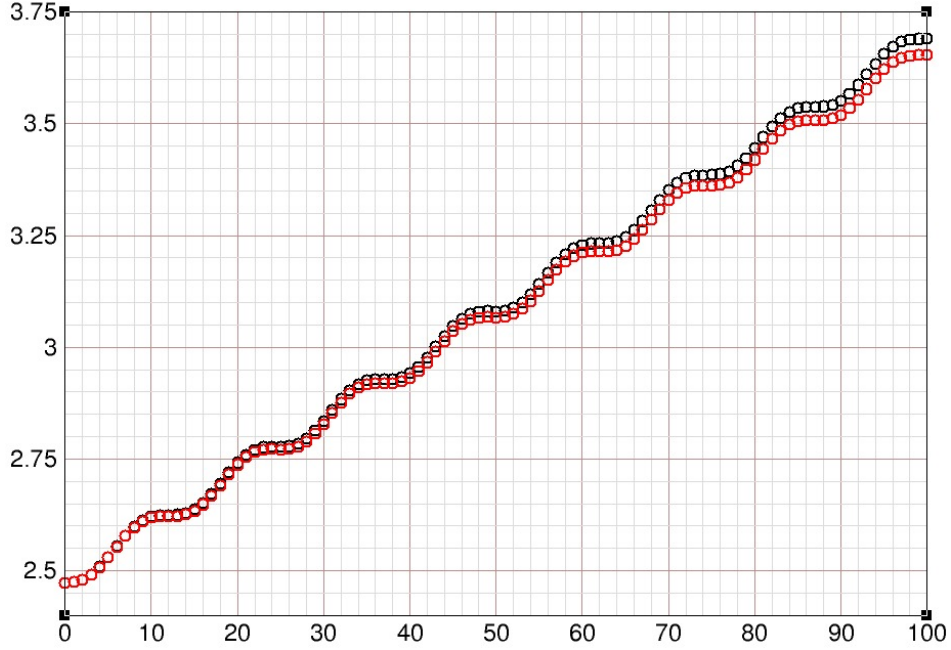


Figure 13: Simulation values of normalized 95% emittance $(6\mathcal{E}_n)_N$ obtained under foil setups 1 (black circles) and 3 (red circles). The setups are defined in Section 2. The horizontal axis gives the turn number n . The units of the vertical axis are μm . The initial normalized 95% emittance is $(6\mathcal{E}_0)_N = 2.47 \mu\text{m}$. The surface density of the carbon foil is 200 microgram per cm^2 . The tune $Q = 0.54$. Under setup 1 all particles pass through the foil on every turn. Under setup 3 the foil extends from $\mathcal{C} - L$ to $\mathcal{C} + L$ where \mathcal{C} is the position of the closed orbit at the foil. It is assumed that the initial beam distribution is centered on the closed orbit. The value of L is set to the initial half-width (4.2 mm) of the beam so that the incoming H-minus beam just fits on the foil. On subsequent turns particles hit the foil only if $-L \leq X_{ni} \leq L$. The emittance growth $(6\mathcal{E}_n - 6\mathcal{E}_0)_N$ over 100 turns is noticeably smaller under setup 3 (red circles). This is quantified for 333 turns in the next figure.

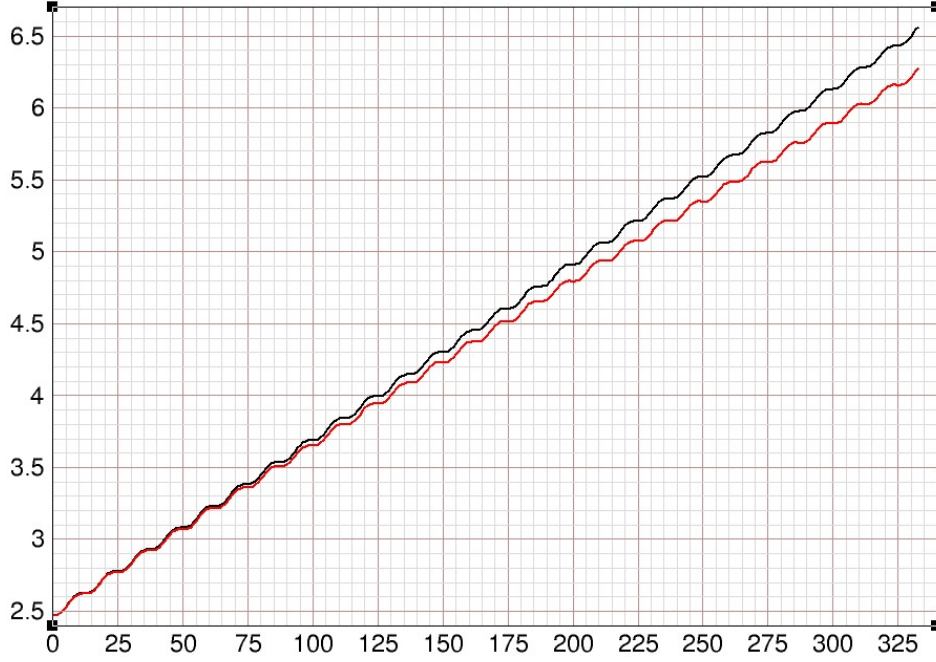


Figure 14: Same as previous figure but with the simulation extended to 333 turns. The values of $(6\mathcal{E}_n)_N$ obtained under foil setups 1 (black curve) and 3 (red curve) are again shown. As before, the horizontal axis gives the turn number n . The units of the vertical axis are μm . The initial normalized 95% emittance is $(6\mathcal{E}_0)_N = 2.47 \mu\text{m}$. The surface density of the carbon foil is 200 microgram per cm^2 . The tune $Q = 0.54$. The emittance growth $(6\mathcal{E}_n - 6\mathcal{E}_0)_N$ obtained over 333 turns under setup 1 is $4.09 \mu\text{m}$. This is reduced to a growth of $3.81 \mu\text{m}$ under setup 3. The reduction of growth therefore amounts to $(4.09 - 3.81)/4.09 = 6.8\%$. Note that except for the small oscillations, the black curve is linear in accordance with (51). The red curve is nonlinear and curves away from the black curve.

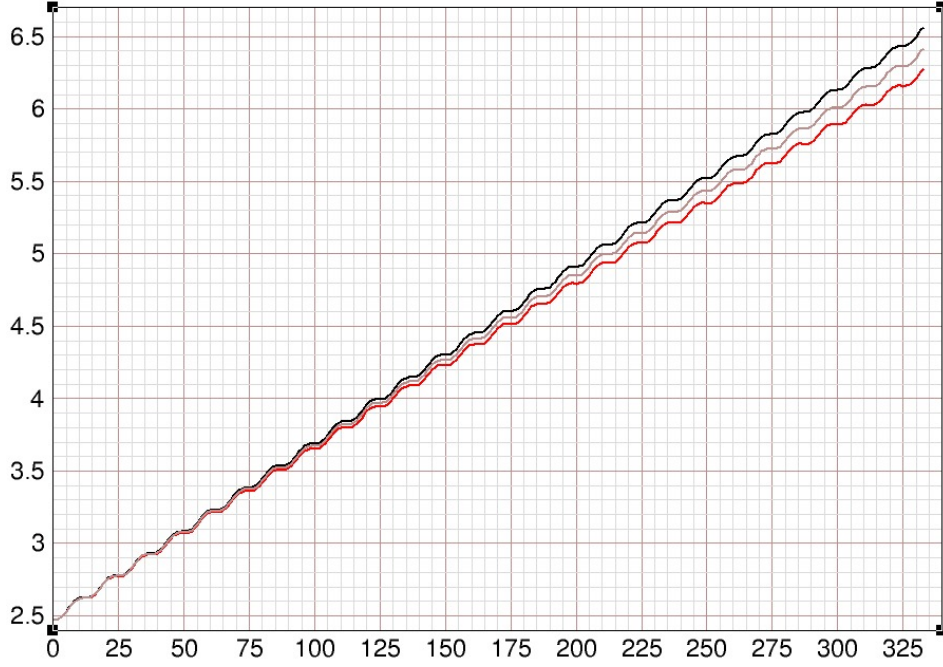


Figure 15: Same as previous figure, but with the addition of $(6\mathcal{E}_n)_N$ obtained under setup 2 (brown curve). Under this setup the foil extends from the beam pipe wall at $-\mathcal{A}$ to $\mathcal{C} + L$, where \mathcal{C} is the position of the closed orbit. It is assumed, as before, that the initial beam distribution is centered on the closed orbit at the foil. The value of L is again set to the initial half-width (4.2 mm) of the beam. This means that the incoming H-minus beam is completely on the foil, but the edge of the beam is up against foil edge. The emittance growth $(6\mathcal{E}_n - 6\mathcal{E}_0)_N$ obtained over 333 turns under this setup is $3.95 \mu\text{m}$. The reduction of growth from that of setup 1 (black curve) therefore amounts to $(4.09 - 3.95)/4.09 = 3.4\%$. This is half the reduction (6.8%) achieved under setup 3 (red curve).

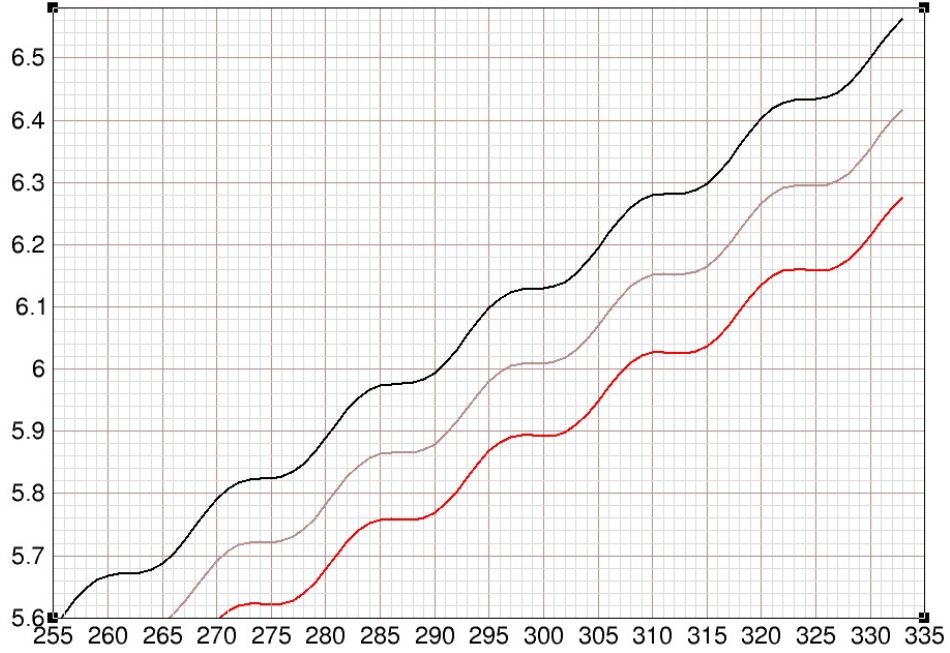


Figure 16: Magnified view of Figure 15. The final normalized 95% emittances $(6\mathcal{E}_n)_N$ obtained after 333 turns under setups 1 (black curve), 2 (brown curve), and 3 (red curve) are 6.56, 6.42, and 6.28 μm respectively. The reduction in final emittance from 6.56 to 6.28 μm amounts to $(6.56 - 6.28)/6.56 = 4.3\%$. The reduction from 6.56 to 6.42 μm amounts to $(6.56 - 6.42)/6.56 = 2.1\%$. Thus, when normalized to the final emittance obtained under setup 1, the reductions obtained under setups 2 and 3 are small.

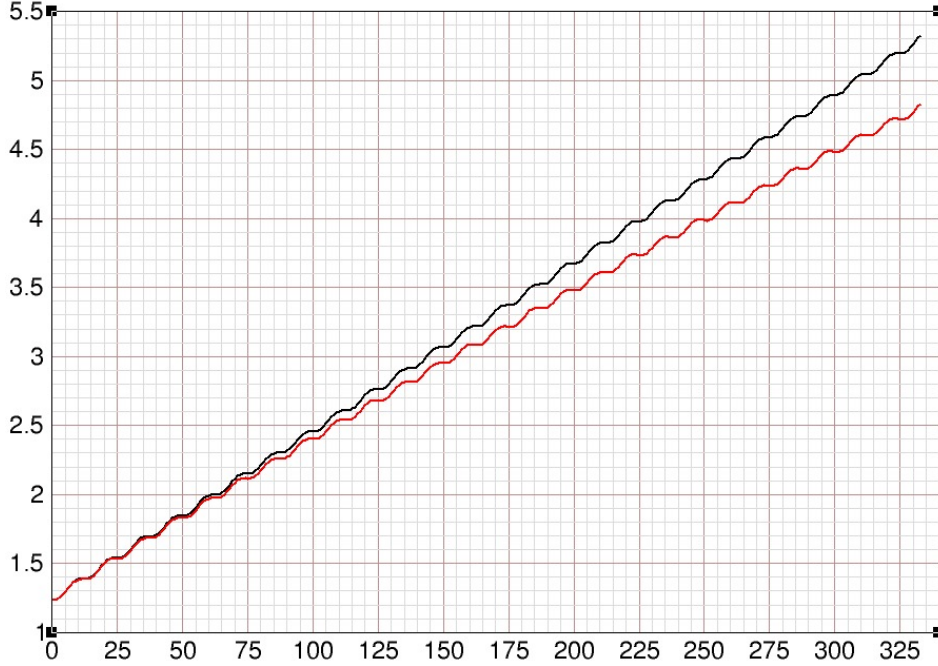


Figure 17: Here and in the next figure we look at the effect of reducing the initial emittance. Simulation values of $(6\mathcal{E}_n)_N$ obtained over 333 turns under foil setups 1 (black curve) and 3 (red curve) are shown. The horizontal axis gives the turn number n . The units of the vertical axis are μm . The tune $Q = 0.54$. Here the initial normalized 95% emittance is **reduced by a factor of two** from $(6\mathcal{E}_0)_N = 2.47$ to $1.24 \mu\text{m}$. The surface density of the carbon foil is again 200 microgram per cm^2 . Under setup 1 the emittance growth $(6\mathcal{E}_n - 6\mathcal{E}_0)_N$ obtained over 333 turns is again $4.09 \mu\text{m}$. Since all particles pass through the foil on every turn under this setup, the growth is independent of the initial emittance as demonstrated in [1]. Under setup 3 the value of L is set to the initial half-width of the beam which is now reduced from 4.2 to 3.0 mm. This gives an emittance growth of $3.59 \mu\text{m}$ over 333 turns. The reduction of growth therefore amounts to $(4.09 - 3.59)/4.09 = 12.2\%$, which is a modest increase from the 6.8% reduction achieved in Figure 14. Note again that the red curve is nonlinear and curves away from the black curve.

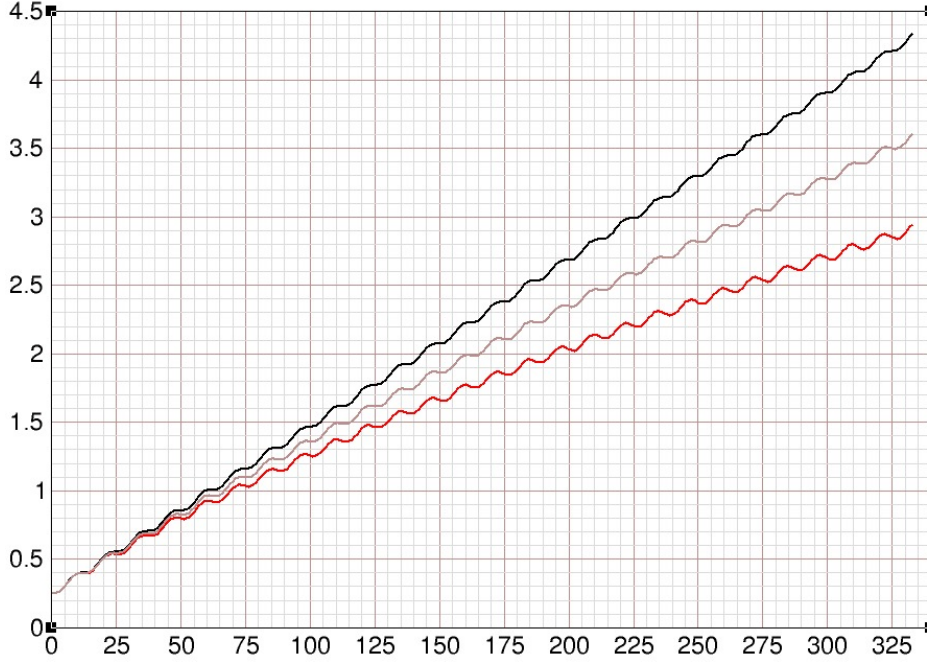


Figure 18: Simulation values of $(6\mathcal{E}_n)_N$ obtained over 333 turns under foil setups 1 (black curve), 2 (brown curve), and 3 (red curve) are shown. The horizontal axis gives the turn number n . The units of the vertical axis are μm . The tune $Q = 0.54$. Here the initial normalized 95% emittance is **reduced by a factor of ten** from $(6\mathcal{E}_0)_N = 2.47$ to $0.247 \mu\text{m}$. The surface density of the carbon foil is again $200 \text{ microgram per cm}^2$. Under setup 1 the emittance growth $(6\mathcal{E}_n - 6\mathcal{E}_0)_N$ obtained over 333 turns is again $4.09 \mu\text{m}$. Under setups 2 and 3 the value of L is set to the initial half-width of the beam which is now reduced from 4.2 to 1.34 mm . This gives emittance growths of $3.36 \mu\text{m}$ and $2.70 \mu\text{m}$ for setups 2 and 3, respectively, over 333 turns. The reductions of growth therefore amount to $(4.09 - 3.36)/4.09 = 18\%$ and $(4.09 - 2.70)/4.09 = 34\%$ which are significant reductions. In this extreme case of very small initial emittance one can say that it does pay to use setups 2 or 3. It is also clear that the brown and red curves are nonlinear and curve away from the black curve.

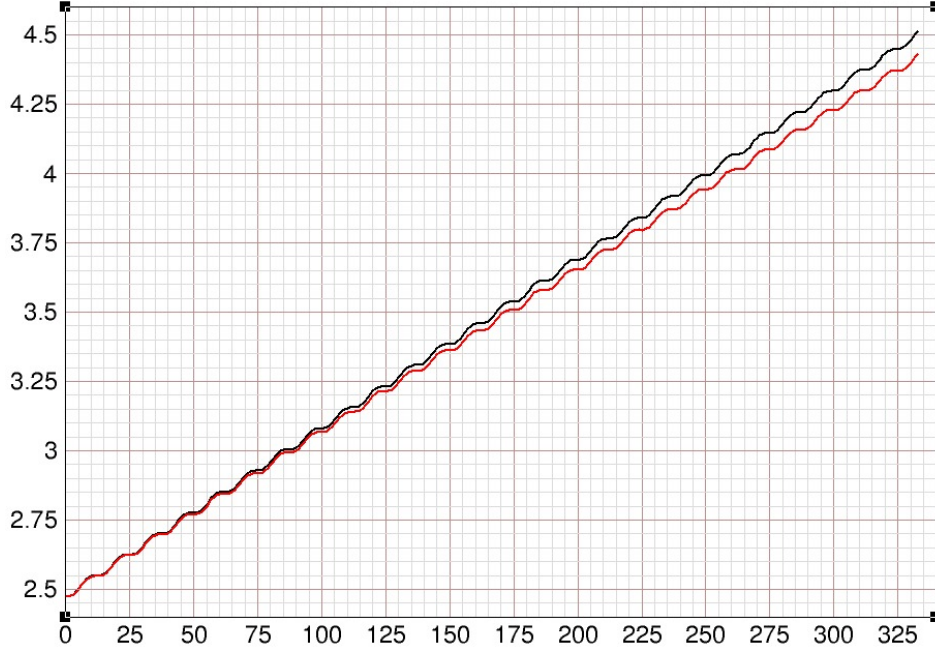


Figure 19: We consider now the case in which the surface density of the carbon foil is reduced from 200 to 100 microgram per cm^2 . This is the surface density routinely used for operation of Booster with polarized protons. Simulation values of $(6\mathcal{E}_n)_N$ obtained under setups 1 (black curve) and 3 (red curve) are shown. The horizontal axis gives the turn number n . The units of the vertical axis are μm . The initial normalized 95% emittance is again $(6\mathcal{E}_0)_N = 2.47 \mu\text{m}$, which is consistent with recent measurements of the Linac beam. The tune $Q = 0.54$. Under setup 1, the emittance growth $(6\mathcal{E}_n - 6\mathcal{E}_0)_N$ obtained over 333 turns is $2.04 \mu\text{m}$, which is half that obtained with the 200 microgram per cm^2 foil. Under setup 3 the growth is reduced to $1.96 \mu\text{m}$. The final emittances $(6\mathcal{E}_n)_N$ obtained under setups 1 and 3 are $4.51 \mu\text{m}$ and $4.43 \mu\text{m}$ respectively. The reduction in final emittance ($4.51 - 4.43 = 0.08 \mu\text{m}$) is therefore small compared to the emittance itself. The conclusion is that the special foil described in setup 3 is not really necessary; an ordinary foil like the one described in setup 2 is all that is needed. This setup has the advantage that with the incoming beam placed up against the foil edge, one can quickly move the circulating proton beam off the foil at the end of H-minus injection.